INVESTIGATION OF THE HYDROGEN EVOLUTION REACTION ON REDUCED AND COBALT-DECORATED TiO_2 NANOTUBES CATALYST IN ALKALINE WATER SPLITTING

Roberta MIFTODE[1], Alexandru MANEA[2], Alexandru MUSTEAȚĂ[2], Mihaela MÎNDROIU[1*]

This study synthesized a hybrid Ti/TiO_2NTr/Co electrocatalyst through the electrochemical reduction of TiO_2 nanotubes followed by cobalt nanoparticle decoration. The reduction process narrowed the bandgap and increased Urbach energy, promoting electron trapping sites that suppress electron-hole recombination and enhance charge transfer. Electrochemical testing in alkaline media demonstrated superior performance for Ti/TiO_2NTr/Co for the hydrogen evolution reaction (HER) compared to untreated TiO_2NT, exhibiting a more electropositive reduction potential, lower overpotential, and reduced charge transfer resistance attributed to the synergistic interaction between the TiO_2NTr matrix and Co nanoparticles. These results underline the potential of this system for advanced energy conversion applications.

Keywords: Ti/TiO_2NTr/Co catalyst; nanotubes; electrochemical reduction; hydrogen evolution reaction; electrocatalytic activity.

1. Introduction

In the 21st century, humanity faces significant challenges, particularly in terms of energy sustainability and environmental conservation. The growing need for energy, coupled with the depletion of limited natural resources, has increased the need to implement sustainable alternatives. A global movement is emerging to connect human activities with ecological principles by promoting awareness of the Earth's limited resources and by adopting responsible consumption practices to maintain long-term economic and ecological stability. A significant problem is the cumulative effect of global pollution and the persistent energy problem, both of which profoundly affect daily life. Rapid industrial growth and population growth in recent decades have intensified these challenges, leading to the development of innovative and sustainable energy production technologies. In this context,

[1]Faculty of Chemical Engineering and Biotechnologies, The National University of Science and Technology POLITEHNICA Bucharest, Romania
[2] Faculty of Power Engineering, The National University of Science and Technology POLITEHNICA Bucharest, Romania
*Corresponding author: mihaela.mindroiu@upb.ro

renewable energy sources have developed as viable alternatives to fossil fuels, offering sustainable solutions for energy production while reducing the impact on the environment. Among these renewable sources, hydrogen stands out due to its advantageous environmental and energy characteristics. Unlike traditional fossil fuels that emit carbon dioxide (CO_2) and contribute substantially to global warming, hydrogen combustion generates only water vapour, thus eliminating greenhouse gas emissions. Furthermore, hydrogen is a clean and renewable energy source with significant potential to reduce pollution and facilitate the development of sustainable energy systems. Global hydrogen production is currently estimated at 87 million tonnes per year, underscoring its growing importance in the transition to a low-carbon economy [1]. Moreover, the hydrogen production through water electrolysis represents an attractive method, that doesn't require sophisticated equipment and doesn't produce additional emissions. The implementation of this method relies heavily on low-cost, high-performance electrocatalysts used in the hydrogen evolution reaction (HER) at the cathode and the oxygen evolution reaction (OER) at the anode [2].

Nanostructured materials has opened significant opportunities in energy conversion and storage by providing unique properties absent in bulk materials, such as high specific surface area, enhanced optical and physical characteristics [3]. These features contribute to superior performance in energy applications, particularly in electrocatalysis for hydrogen production via water electrolysis, where nanostructures could facilitate the rapid charge transfer and increase the number of active reaction sites. Titanium dioxide (TiO_2) is a widely used semiconductor in energy applications due to its better contact surface and the presence of pairs of electron holes that enhance electron transport, photocatalytic properties, and stability [4]. Nanostructured TiO_2 is employed in lithium-ion batteries, dye-sensitized solar cells, fuel cells, and supercapacitors. Among these, TiO_2 nanotubes, are particularly advantageous for photocatalytic and electrocatalytic applications due to their one-dimensional morphology, which promotes efficient charge transport and provides a large surface area [5].

However, TiO_2 has two major limitations: a wide band gap (3.2 eV for anatase phase) that restricts its light absorption to the UV spectrum and a high recombination rate of photogenerated electron-hole pairs that reduces its catalytic efficiency. To overcome these limitations, oxygen vacancies are deliberately introduced into the TiO_2 structure via an electrochemical reduction process. These vacancies create intermediate energy states that narrow the band gap and enhance the material's ability to absorb light in the visible spectrum [6,7].

In addition, TiO_2 doping by transition metals such as Co further enhances its properties by changing its electronic structure and creating additional oxygen vacancies. These defects introduce intermediate energy states that reduce the band gap while maintaining the charge neutrality. The combination of the titania

electrochemical reduction and its cobalt doping synergistically improves the electrocatalytic performance of the final nanostructured material by enhancing its conductivity, suppressing charge recombination, and providing more active catalytic sites, thus enhancing the physical properties and photocatalytic activity of TiO_2 [8].

This study presents experimental results related to the development of a novel electrocatalyst based on cobalt decorated-electrochemically reduced TiO_2 nanotubes. This dual modification strategy aims to overcome the intrinsic limitations of TiO_2 by reducing its band gap, increasing Urbach energy, creating electron-trapping sites to suppress recombination, and improving the charge transfer efficiency. The preliminary results demonstrate that the new catalyst exhibits superior electrocatalytic activity towards hydrogen evolution reaction in alkaline solutions compared to pristine TiO_2 nanotubes, exhibiting higher electropositive reduction potential, lower overpotential, reduced charge transfer resistance, and an optimized active surface area. This approach highlights the potential of advanced nanostructured materials for efficient hydrogen production via water electrolysis.

2. Experimental

2.1. Materials

Ammonium fluoride (NH_4F) (Sigma Aldrich), sodium sulphate (Na_2SO_4), ethylene glycol ($C_2H_6O_2$) (EG) (Honeywell, Charlotte, NC, USA, $\geq$ 99.5%), cobalt nitrate ($Co(NO_3)_2 \cdot 6H_2O$) (Sigma Aldrich), nitric acid (HNO_3) has been used as received.

2.2. Preparation of reduced and cobalt-decorated TiO_2 nanotubes (Ti/TiO_2NTr/Co) on a titanium substrate

In the first step, TiO_2 nanotubes were produced using anodization technique. Initially, 99.6% pure Ti samples (provided by Goodfellow) were polished with abrasive papers of various granulometry (Carbimet, Buehler), then cleaned with distilled water and degreased in ethanol and acetone at ambient temperature. The electrochemical cell used for anodization consisted of a Ti electrode as the anode and a platinum electrode as the cathode, with an electrolyte solution made up of 0.5% wt NH_4F and 2% vol. distilled water in EG solution. Using a MATRIX MPS-7163 source, the voltage was raised from 0 to 60V with a rate of 2 V/10 s then maintained constant at room temperature for 2 hours.

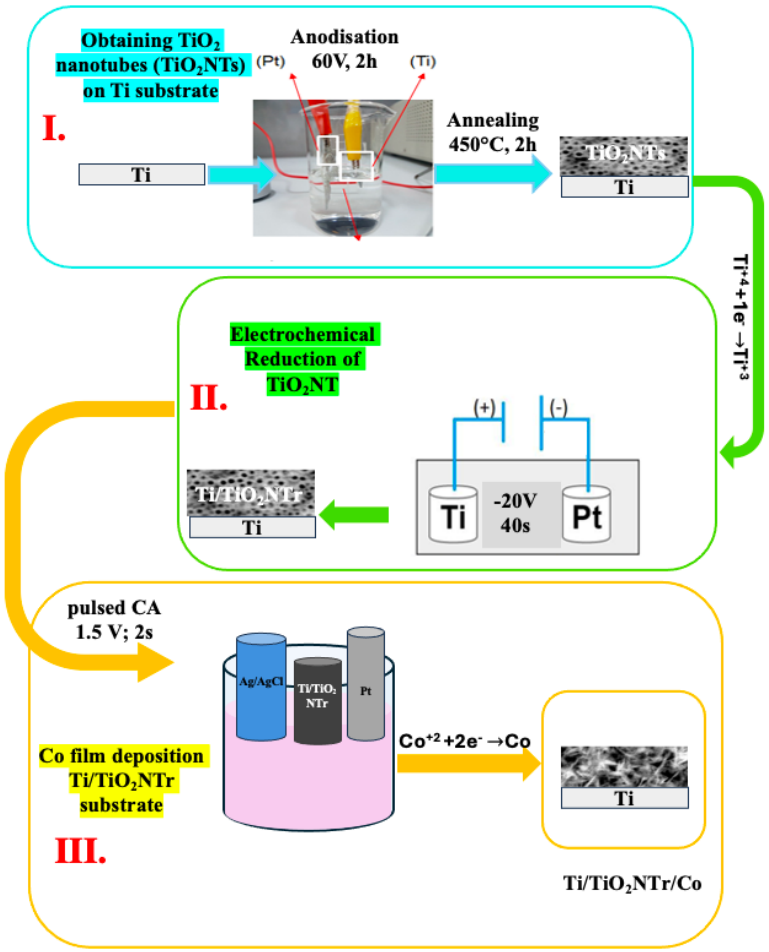

Fig. 1. The process flow of the Ti/TiO_2NTr/Co electrode preparation

Then, the sample was calcined in an oven set to 450 °C for 2 hours, and **Ti/TiO_2NT** electrode was obtained.

Fig. 1 illustrates the overall catalyst preparation process flow, including the next steps that are described in the paragraphs below.

In the second step, TiO_2NT film was electrochemically reduced to produce defects in the TiO_2 film lattice, such as oxygen vacancies (O_v) and/or Ti^{3+} centres by reducing Ti^{4+} to Ti^{3+} ($Ti^{4+} + e^- \rightarrow Ti^{3+} + 1/2O_2\uparrow$) [9,10]. A solution containing 1 g of Na_2SO_4 dissolved in 15 g of deionised water and 234 g of ethylene glycol [11], was used. A platinum counter electrode and one working Ti/TiO_2NT electrode were employed. The electrochemical reduction was conducted by applying a potential of -20 V for 40 seconds using an EA-PS 3200-04C power source. The reduced sample was named **Ti/TiO_2NTr**.

In the third step, the pulsed chronoamperometry technique was applied for the electrochemical deposition of cobalt, according to our previous study [12]. The Ti/TiO_2NTr electrode served as the working electrode, immersed in an aqueous solution composed of a mixture of $Co(NO_3)_2$ and HNO_3 in 1:1 molar ratio (pH = 4), while Ag/AgCl, KCl sat. acted as the reference electrode, and Pt mesh as the counter electrode. A Metrohm (Herisau, Switzerland) Autolab (PGSTAT 302N) potentiostat/galvanostat was employed to control parameters and acquire the data.

Three stages were performed for the formation of the **Ti/TiO_2NTr/Co** electrode: (i) applying −1.5 V for 2 seconds to start the Co nucleation on the TiO_2NTr substrate; (ii) keeping the open circuit voltage for 5 seconds; (iii) thereafter applying −0.95 V for 5 seconds to initiate Co deposition. Stages (ii) and (iii) were repeated for 200 times.

2.3. Characterization

The optical properties

The bandgap energy (E_g) and Urbach energy (E_u) were determined through UV-Vis transmittance measurements across the 300–800 nm wavelength range using a PerkinElmer Lambda 850 UV/Vis spectrophotometer.

Physicochemical characterization

To investigate the film's morphology, the QUANTA INSPECT F50 scanning electron microscope (FEI Company, Eindhoven, The Netherlands) was used, equipped with a field emission gun (FEG) offering a resolution of 1.2 nm. The contact angle measurements have completed the surface characterization, to quantify the wettability of a solid surface by a liquid and to calculate the surface free energy (SFE). To determine the surface free energy, the sessile drop method was employed to measure the contact angles using an optical contact angle goniometer (Contact Angle Meter – KSV Instruments CAM 100) equipped with a camera. Three different probe liquids were used: distilled water, ethylene glycol (EG), and dimethyl sulfoxide (DMSO). The surface energy was calculated using the Owens-Wendt model (OW), which is based on contact angle measurements [13]. The total surface free energy (γ_{SV}) is calculated using the following equation:

$$\gamma_{SV} = \gamma_{SV}^{d} + \gamma_{SV}^{p}, \tag{1}$$

where γ^{d}_{SV} is dispersive component (Lifshitz–Van der Waals interactions) and γ^{p}_{SV} is non-dispersive component (polar interactions, Lewis acid–base). The Young equation was used to correlate the interfacial tensions $(\gamma_{SV}, \gamma_{SL}, \gamma_{LV})$ to the contact angle (θ):

$$-\gamma_{SV} + \gamma_{SL} + \gamma_{LV} \cdot \cos\theta = 0 \tag{2}$$

The equation relating tension components to contact angle utilised in the OW model is:

$$\gamma_{LV} \cdot (1 + \cos\theta) = \sqrt[2]{\left(\gamma_{SV}^{d} \cdot \gamma_{LV}^{d}\right)} + \sqrt[2]{\left(\gamma_{SV}^{p} \cdot \gamma_{LV}^{p}\right)} \quad (3)$$

Electrochemical characterization

Moreover, the electrocatalytic activity (EA) of the Ti/TiO_2NTr/Co catalyst for the HER activity was evaluated using an EA cell, which included a three-electrode setup connected to an Autolab (PGSTAT 204) potentiostat/galvanostat from Metrohm (Herisau, Switzerland), controlled by Nova software. To ensure reproducibility, three Ti/TiO_2NTr/Co electrodes were used as working electrodes, each with a geometrical surface area of 16 cm^2. A platinum wire and Ag/AgCl, KCl sat. electrode were used as the counter and reference electrodes, respectively. Advanced techniques were employed, including linear sweep voltammetry (LSV) and electrochemical impedance spectroscopy (EIS) to evaluate electrocatalytic activity. EA measurements were performed in 1 M KOH solution at pH = 13. LSV curves were obtained with a scan rate of 5 mV/s in the potential domain of 0.2 V and -1 V, and the calculated overpotential values are an average of three scans for each electrode. EIS measurement was conducted in the frequency range of 100 kHz to 0.01 Hz with an AC amplitude of ± 5 mV signal at the open circuit potential. All potentials were referenced to a reversible hydrogen electrode (RHE), with the Ag/AgCl reference electrode calibrated accordingly. The RHE potential (E_{RHE}) was determined using the equation: $E_{RHE} = E_{Ag/\ AgCl} + 0.241 + 0.059 \cdot pH$.

3. Results and discussion

3.1. Scanning electron microscopy

Fig. 2 illustrates SEM images captured at different magnifications to examine the Ti/TiO_2NTr and Ti/TiO_2NTr/Co structure. Fig. 2a depicts the nanotube shape of the TiO_2 film formed during electrochemical anodization on titanium substrate. Fig. 2b shows that cobalt decoration of TiO_2NTr film leads to the development of star-shaped nanostructures. A homogeneous electrochemically deposited Co layer was obtained on the entire surface.

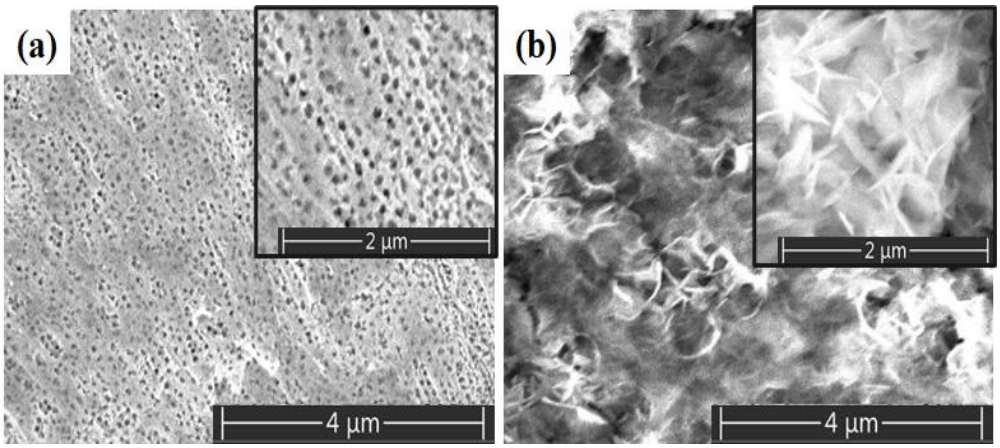

Fig. 2. SEM images recorded at various magnifications for (a) Ti/TiO_2NTr; (b) Ti/TiO_2NTr/Co

3.2. Contact angle measurement - wettability and surface free energy (SFE)

The level of wettability and the SFE value determine the surface HER performance of TiO_2NT based catalysts. Through their effects on electrolyte accessibility, mass transfer, gas bubble adhesion, and catalyst degradation, these parameters have a major impact on the kinetics and efficiency of the hydrogen evolution reaction [14].

The electrodeposition of TiO_2 nanotubes improves the wettability of the titanium electrode, as shown in Fig. 3a, with the contact angle measured against H_2O decreasing from 60 degrees to approximately 19 degrees.

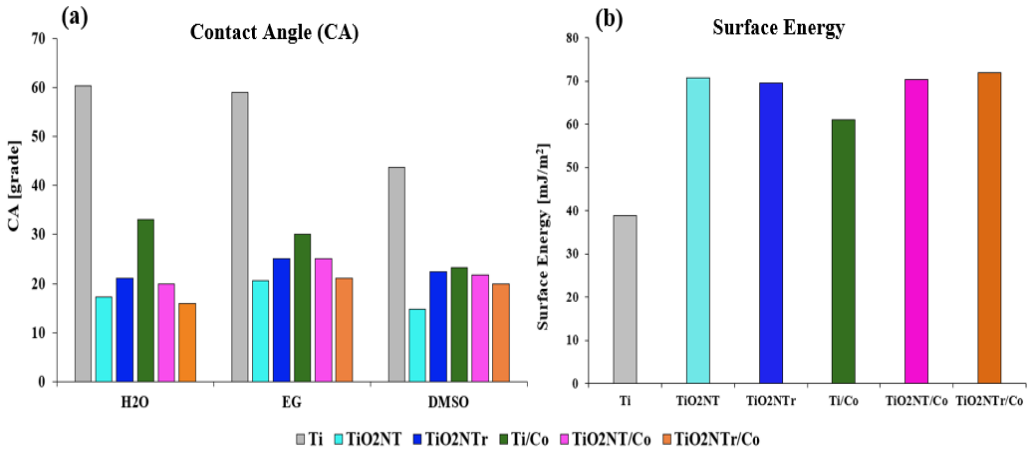

Fig. 3. The contact angle (a) and surface free energy values (b) for the obtained catalyst

A similar behaviour was observed for the other two electrolytes (EG and DMSO) used to measure the contact angle for determining the surface free energy. Furthermore, all the investigated surfaces display enhanced wettability.
Both the reduction treatment and the subsequent decoration with Co, with the star-like morphology of the Ti/TiO_2NTs substrate, further improve the wettability compared to titanium electrode. As illustrated in Fig. 3b, the surface free energy (SFE) of TiO_2-based films varies depending on the applied treatments, such as thermal reduction and cobalt decoration.

This behaviour can be attributed to the generation of surface defects and changes in surface chemistry [15]. The Owens-Wendt-Rabel-Kaelble (OWRK) model was successfully employed to calculate the surface free energy values [16]. An increase in SFE correlates with a reduction in contact angle values, facilitating enhanced H^+ ion adsorption on the catalyst surface and promoting the desorption of reaction intermediates and products, thereby improving the overall efficiency of the hydrogen evolution reaction (HER) [14].

3.3. The impact of the band gap and Urbach energy values on the efficiency of the Hydrogen Evolution Reaction (HER)

Fig. 4 depicts the plot of $(\alpha h\nu)^2$ versus hν (Fig. 4a) and the graph of ln(α) as a function of photon energy (Fig. 4b) for all electrocatalysts, with and without cobalt decoration, were E_g is the band-gap energy, hν is the energy of the incident photon [17] and α is the absorption coefficient [18]. The band gap and Urbach energies were estimated using Tauc's equation and from the graph ln(α) = f (photon energy), respectively, according to our previous work [19]. The band gap for the Ti/TiO_2NT electrode has the highest value, E_g = 3.16 eV, as shown in Fig. 4a.

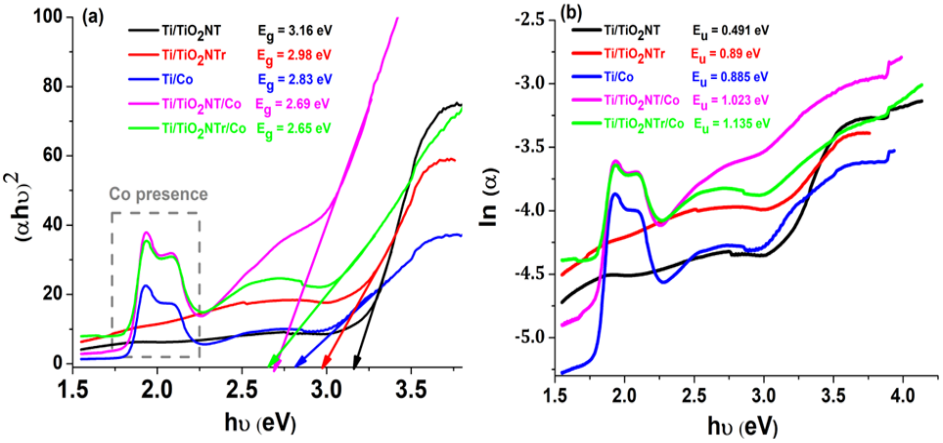

Fig. 4. (a) plot of $(\alpha h\nu)^2$ versus hν and (b) ln(α) versus photon energy plots for obtained electrocatalysts

This is due to the fact that following the treatment the Ti^{4+} cations were reduced to Ti^{3+} [21], which act as defects below the conduction band of the TiO_2NTr lattice [9,10]. As a result, these defects can trap electrons, significantly lowering the energy needed to excite an electron from the valence band (VB) to the conduction band (CB) and the rate at which electrons and holes recombine. This process promotes the transport of charge to the surface for the HER reaction [22]. The decoration of TiO_2NTr with cobalt significantly reduces the band gap to E_g = 2.67 eV, suggesting a modification of the electronic structure. A Schottky heterojunction between TiO_2NTr and Co is created, which improves charge separation and the transfer of electrons to water to generate hydrogen [23,24].

The presence of lattice defects in the TiO_2NTr/Co film is indicated by a notable Urbach energy associated with an extended tail band, as documented in the literature [10,25]. Fig. 4b illustrates a significant rise in Urbach energy values, increasing from 0.491 eV for the TiO_2NT film to 1.135 eV for TiO_2NTr/Co.

Consequently, we can deduce that implementing a reduction treatment and creating a Schottky heterojunction between TiO_2NTr and Co enhances the presence of localised defects (in the form of Ti^{3+} centres) beneath the conduction band, facilitating the transfer of electrons to water for hydrogen production [26,27].

3.4. The electrochemical activity of the prepared Ti/TiO_2NTr/Co catalyst for the HER

Fig. 5 presents the linear sweep voltammetry (LSV) curves of the obtained electrocatalysts: Ti/TiO_2NT, Ti/TiO_2NTr, Ti/TiO_2NT/Co, and Ti/TiO_2NTr/Co, highlighting their electrocatalytic activity toward the hydrogen evolution reaction (HER).

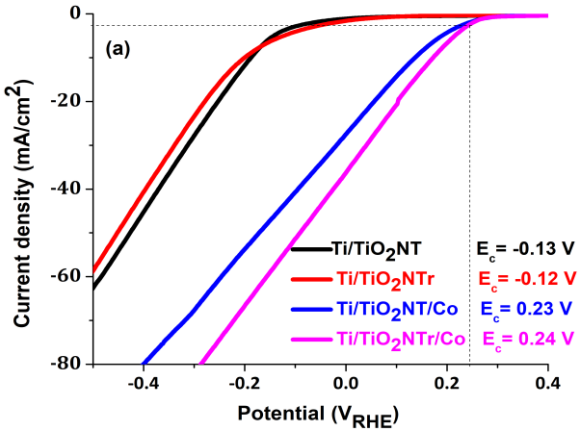

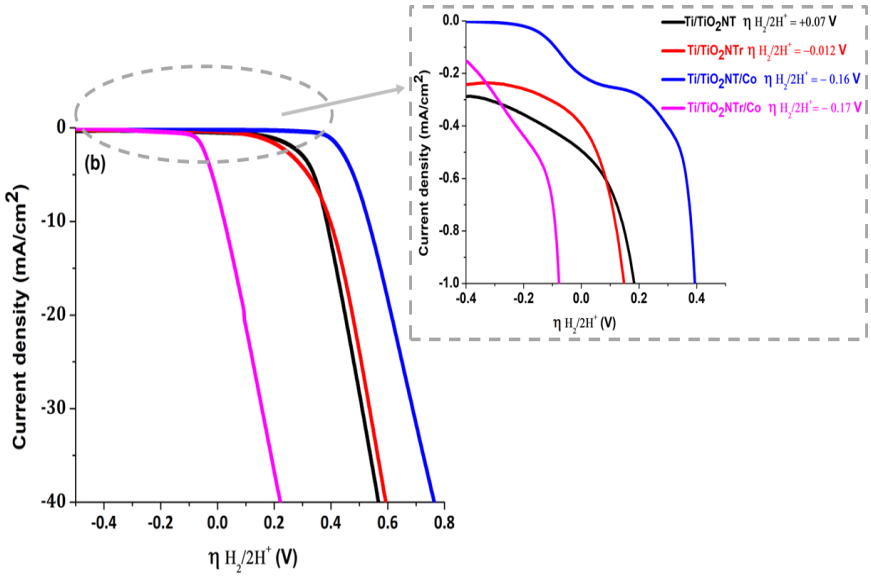

Fig. 5. Cathodic current vs. (a) electrode potential ($E_{(RHE)}$), and (b) hydrogen evolution reaction overvoltage ($\eta_{H2/2H+}$), recorded in 1 M KOH solution (pH 13) at a scan rate of 5 mV·s^{-}

Fig. 5a illustrates that the Ti/TiO$_2$NTr/Co electrocatalyst exhibits the most positive cathodic potential (E_c = 0.24 V vs. RHE) and the highest current density, indicating a strong intrinsic catalytic activity. The improvement is due to the formation of the Schottky heterojunction at the TiO$_2$NT/Co interface, the formation of Ti^{3+} surface defects generated by the electrochemical reduction treatment, a decrease in the electron-hole recombination rate, and the increased surface wettability attributed to the star-shaped morphology of cobalt.

In Fig. 5b the catalytic efficiency was evaluated in relation to the HER overpotential values ($\eta_{H2/2H+}$). The Ti/TiO$_2$NTr/Co electrocatalyst exhibits a low energy barrier for the hydrogen evolution process, characterised by its low overpotential (-0.17 V ± 0.002) at a current density near zero. In contrast, the Ti/TiO$_2$NT electrode exhibits an increased overpotential (+0.07 V ± 0.0042), which was diminished by applying the reduction treatment (-0.012 V ± 0.0004) and/or cobalt decoration (-0.16 V ± 0.0025). These results indicate that the integration of the electrochemical reduction treatment with cobalt decoration provides a synergistic effect, enhancing the kinetics of the HER. Together with the low charge transfer resistance shown by the EIS data, the low overpotential suggests effective electron transfer and reduced electron-hole recombination losses, which enhances hydrogen production on the Ti/TiO$_2$NTr/Co electrocatalyst surface.

Fig. 6 displays the Nyquist plots from electrochemical impedance spectroscopy (EIS) for the studied electrocatalysts.

The charge transfer resistance (R_{ct}) value directly influences the HER efficiency and was measured from the EIS spectra at the catalyst/alkaline solution interface.

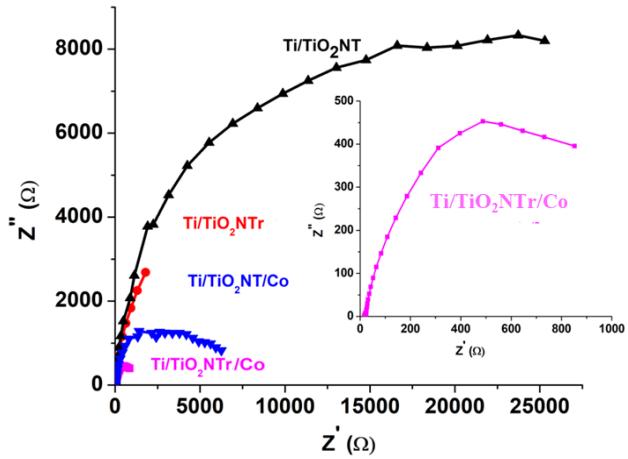

Fig. 6. Nyquist plots of EIS measurements recorded in 1M KOH solution in the frequency range of 100 kHz to 0.01 Hz at the open circuit potential

Fig. 6 showed that the Ti/TiO_2NT catalyst has the highest R_{ct} value (50 kΩ), indicating slow electron transfer kinetics and limited surface charge transport. However, by reducing the TiO_2NT layer, the arc diameter in the Nyquist diagram decreases, suggesting that conductivity increases when defects emerge in the TiO_2NT network. The Ti/TiO_2NT/Co electrocatalyst exhibits a significantly smaller arc, suggesting that by decorating with cobalt the charge transfer and electrical conductivity have been improved.

According to the EIS analysis, these results show that Ti/TiO_2NTr/Co has the best electrocatalytic behaviour among all the catalysts studied.

In Fig. 7 it was proposed the mechanism for water splitting in an alkaline solution (1 M KOH, pH=13) using Ti/TiO_2NTr/Co catalyst with abundant defects due to the synergistic effect of Co decoration and electrochemical reduction of TiO_2 nanotubes.

By applying a voltage to the EA cell, where the Ti/TiO_2NTr/Co electrode is the cathode, the electrons from the valence band (VB) excite to the conduction band (CB), generating electron-hole pairs (e^--h^+), according to the reaction: (TiO_2NTr/Co + e^- → TiO_2NTr/Co (e^-) + h^+). In the EA cell, the following reactions occur: at the cathode, the electrons react with water to produce hydrogen gas (H_2) ($4H_2O + 4e^- \rightarrow 2H_2\uparrow + 4OH^-$), while at the anode (platinum), hydroxide ions (OH^-) react with the holes to release oxygen (O_2) ($4OH^- + 4\ h^+ \rightarrow O_2\uparrow + 2H_2O + 4e^-$) [28].

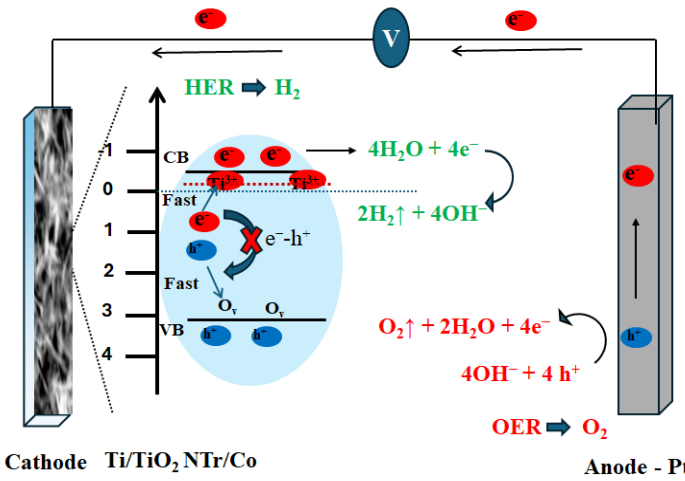

Fig. 7. Schematic diagram of the proposed mechanism for electrochemical splitting water using Ti/TiO₂NTr/Co electrode for the HER in 1 M KOH solution

The presence of the defects in TiO₂NTr/Co lattice, such as oxygen vacancy (O_v) and Ti^{+3} centres which can trap electrons [29], enhances charge separation and catalytic activity, improving the HER at the cathode. These defects narrow the bandgap, increase the Urbach energy and increase conductivity, and reduce electron-hole recombination, directly contributing to enhanced hydrogen evolution.

4. Conclusions

The performance of hydrogen evolution reaction (HER) catalysts composed of TiO_2 nanotubes on titanium electrodes was improved by an electrochemical reduction treatment followed by the formation of a Schottky heterojunction by cobalt decoration using a simple pulsed electrochemical method. According to the morphological data, a cobalt film with a star-shaped morphology was deposited on the surface of the TiO₂NTr nanostructures. This film had a high surface energy and good wettability, which sustained a good adsorption of H^+ ions on the catalytic surface.

The cobalt decoration and electrochemical reduction treatment promoted the formation of localised defects below the conduction band of the TiO₂NT film, which facilitates the transfer of electrons to water for hydrogen production. With a high Urbach energy and the lowest band gap, the Ti/TiO₂NTr/Co electrocatalyst showed a significant defect density, which led to a decrease in the rate of electrons - holes recombination. This effect is also confirmed by the low charge transfer resistance observed in EIS measurements, which facilitates efficient charge transport to the surface during the HER process. Compared to the Ti/TiO₂NT

electrode without cobalt and without electrochemical reduction, the Ti/TiO_2NTr/Co electrocatalyst has the best catalytic activity for the HER reaction, according to LSV analyses. This is due to the much more active surface, the lower band gap, and the best wettability, which indicates improved surface contact, the lowest overpotential, and the lower charge transfer resistance. In the future, we will use this catalyst as a cathode to eventually create a bifunctional photocatalytic fuel cell.

REFERENCES

1. Shiva Kumar, S.; Lim, H. An overview of water electrolysis technologies for green hydrogen production. Energy Reports **2022**, 8, 13793-13813, doi:https://doi.org/10.1016/j.egyr.2022.10.127.
2. Dong, Z.; Qin, D.; Ma, J.; Li, Z.; Han, S. Bulk-phase and surface dual-defective engineering enabled Ti-based nanotubes photoanode for highly efficient photoelectrochemical water splitting. Renewable Energy **2024**, 231, 121004, doi:https://doi.org/10.1016/j.renene.2024.121004.
3. Weng, Z.; Guo, H.; Liu, X.; Wu, S.; Yeung, K.W.K.; Chu, P.K. Nanostructured TiO2 for energy conversion and storage. RSC Advances **2013**, 3, 24758-24775, doi:10.1039/C3RA44031A.
4. Sassi, S.; Bouich, A.; Bessais, B.; Khezami, L.; Soucase, B.M.; Hajjaji, A. Comparative Analysis of Anodized TiO2 Nanotubes and Hydrothermally Synthesized TiO2 Nanotubes: Morphological, Structural, and Photoelectrochemical Properties. Materials **2024**, 17, doi:10.3390/ma17215182.
5. Nyankson, E.; Agyei-Tuffour, B.; Asare, J.; Annan, E.; Rwenyagila, E.R.; Konadu, D.; Yaya, A.; Dodoo Arhin, D. Nanostructured TiO2 and their energy applications-a review. ARPN Journal of Engineering and Applied Sciences **2013**, 8, 871-886.
6. Kang, Q.; Cao, J.; Zhang, Y.; Liu, L.; Xu, H.; Ye, J. Reduced TiO2 nanotube arrays for photoelectrochemical water splitting. J. Mater. Chem. A **2013**, 1, 5766-5774, doi:10.1039/C3TA10689F.
7. Gao, J.; Shen, Q.; Guan, R.; Xue, J.; Liu, X.; Jia, H.; Li, Q.; Wu, Y. Oxygen vacancy self-doped black TiO2 nanotube arrays by aluminothermic reduction for photocatalytic CO2 reduction under visible light illumination. Journal of CO2 Utilization **2020**, 35, 205-215, doi:https://doi.org/10.1016/j.jcou.2019.09.016.
8. Safeen, A.; Safeen, K.; Ullah, R.; Zulfqar; Shah, W.H.; Zaman, Q.; Althubeiti, K.; Al Otaibi, S.; Rahman, N.; Iqbal, S.; et al. Enhancing the physical properties and photocatalytic activity of TiO2 nanoparticles via cobalt doping. RSC Advances **2022**, 12, 15767-15774, doi:https://doi.org/10.1039/d2ra01948e.
9. Zhou, T.; Li, L.; Li, J.; Wang, J.; Bai, J.; Xia, L.; Xu, Q.; Zhou, B. Electrochemically reduced TiO2 photoanode coupled with oxygen vacancy-rich carbon quantum dots for synergistically improving photoelectrochemical performance. Chemical Engineering Journal **2021**, 425, 131770, doi:https://doi.org/10.1016/j.cej.2021.131770.
10. Mesoudy, A.E.; Machon, D.; Ruediger, A.; Jaouad, A.; Alibart, F.; Ecoffey, S.; Drouin, D. Band gap narrowing induced by oxygen vacancies in reactively sputtered TiO2 thin films. Thin Solid Films **2023**, 769, 139737, doi:https://doi.org/10.1016/j.tsf.2023.139737.
11. Cheng, Y.; Gao, J.; Shi, Q.; Li, Z.; Huang, W. In situ electrochemical reduced Au loaded black TiO2 nanotubes for visible light photocatalysis. Journal of Alloys and Compounds **2022**, 901, 163562, doi:https://doi.org/10.1016/j.jallcom.2021.163562.
12. Irodia, R.; Ungureanu, C.; Sătulu, V.; Mîndroiu, V.M. Photocatalyst Based on Nanostructured TiO2 with Improved Photocatalytic and Antibacterial Properties. Materials **2023**, 16, doi:10.3390/ma16247509.
13. Ungureanu, C.; Dumitriu, C.; Popescu, S.; Enculescu, M.; Tofan, V.; Popescu, M.; Pirvu, C. Enhancing antimicrobial activity of TiO2/Ti by torularhodin bioinspired surface modification. Bioelectrochemistry **2016**, 107, 14-24, doi:https://doi.org/10.1016/j.bioelechem.2015.09.001.

14. Wei, M.; Kuang, Y.; Duan, Z.; Li, H. The crucial role of catalyst wettability for hydrogenation of biomass and carbon dioxide over heterogeneous catalysts. Cell Reports Physical Science **2023**, 4, 101340, doi:https://doi.org/10.1016/j.xcrp.2023.101340.
15. Mahadik, S.A.; Yadav, H.M.; Mahadik, S.S. Surface properties of chlorophyll-a sensitized TiO2 nanorods for dye-sensitized solar cells applications. Colloid and Interface Science Communications **2022**, 46, 100558, doi:https://doi.org/10.1016/j.colcom.2021.100558.
16. Peng, Z.; Ni, J. Surface properties and bioactivity of TiO2 nanotube array prepared by two-step anodic oxidation for biomedical applications. Royal Society open science **2019**, 6, 181948.
17. Landi Júnior, S.; Rocha Segundo, I.; Afonso, C.; Lima Jr, O.; Costa, M.; Freitas, E.; Carneiro, J.O. Evaluation of band gap energy of TiO2 precipitated from titanium sulphate. Physica B: Condensed Matter **2022**, 639, 414008, doi:10.1016/j.physb.2022.414008.
18. Derbali, A.; Attaf, A.; Saidi, H.; Benamra, H.; Nouadji, M.; Aida, M.S.; Attaf, N.; Ezzaouia, H. Investigation of structural, optical and electrical properties of ZnS thin films prepared by ultrasonic spray technique for photovoltaic applications. Optik **2018**, 154, 286-293, doi:https://doi.org/10.1016/j.ijleo.2017.10.034.
19. Mîndroiu, V.M.; Stoian, A.B.; Irodia, R.; Truşcă, R.; Vasile, E. Titanium Dioxide Thin Films Produced on FTO Substrate Using the Sol–Gel Process: The Effect of the Dispersant on Optical, Surface and Electrochemical Features. Materials **2023**, 16, doi:10.3390/ma16083147.
20. Nunes, D.; Freire, T.; Barranger, A.; Vieira, J.; Matias, M.; Pereira, S.; Pimentel, A.; Cordeiro, N.J.; Fortunato, E.; Martins, R. TiO2 nanostructured films for electrochromic paper based-devices. Applied Sciences **2020**, 10, 1200.
21. Xiong, L.-B.; Li, J.-L.; Yang, B.; Yu, Y. Ti3+ in the surface of titanium dioxide: generation, properties and photocatalytic application. J. Nanomaterials **2012**, 2012, Article 9, doi:10.1155/2012/831524.
22. Hou, X.; Aitola, K.; Jiang, H.; Lund, P.D.; Li, Y. Reduced TiO2 nanotube array as an excellent cathode for hydrogen evolution reaction in alkaline solution. Catalysis Today **2021**.
23. Kumar, V.; Prasad Singh, G.; Kumar, M.; Kumar, A.; Singh, P.; Ansu, A.K.; Sharma, A.; Alam, T.; Yadav, A.S.; Dobrotă, D. Nanocomposite Marvels: Unveiling Breakthroughs in Photocatalytic Water Splitting for Enhanced Hydrogen Evolution. ACS Omega **2024**, 9, 6147-6164, doi:10.1021/acsomega.3c07822.
24. Amna Rambey, M.; Moridon, S.; Arifin, K.; Jeffery Minggu, L.; Kassim, M. Composite of Titanium Dioxide Nanotube and Cobalt Sulfide for Photoelectrochemical Application. Sains Malaysiana **2023**, 52, 2407-2418, doi:10.17576/jsm-2023-5208-17.
25. Choudhury, B.; Choudhury, A. Oxygen defect dependent variation of band gap, Urbach energy and luminescence property of anatase, anatase–rutile mixed phase and of rutile phases of TiO2 nanoparticles. Physica E: Low-dimensional Systems and Nanostructures **2014**, 56, 364-371, doi:https://doi.org/10.1016/j.physe.2013.10.014.
26. Li, J.; Zhang, M.; Guan, Z.; Li, Q.; He, C.; Yang, J. Synergistic effect of surface and bulk single-electron-trapped oxygen vacancy of TiO2 in the photocatalytic reduction of CO2. Applied Catalysis B: Environmental **2017**, 206, 300-307, doi:https://doi.org/10.1016/j.apcatb.2017.01.025.
27. Cui, H.; Zhao, W.; Yang, C.; Yin, H.; Lin, T.; Shan, Y.; Xie, Y.; Gu, H.; Huang, F. Black TiO2 nanotube arrays for high-efficiency photoelectrochemical water-splitting. J. Mater. Chem. A **2014**, 2, doi:10.1039/C4TA00176A.
28. Abass, N.A.; Qahtan, T.F.; Alansi, A.M.; Bubshait, A.; Alwadei, Y.A.; Basiry, N.A.; Albu, Z.; Alhakami, F.S.; Saleh, T.A. Black TiO2 nanotube arrays: Bifunctional electrocatalytic performance for alkaline water splitting. Fuel **2025**, 388, 134300, doi:https://doi.org/10.1016/j.fuel.2025.134300.
29. Xiong, L.-B.; Li, J.-L.; Yang, B.; Yu, Y. Ti3+ in the Surface of Titanium Dioxide: Generation, Properties and Photocatalytic Application. Journal of Nanomaterials **2012**, 2012, 831524, doi:https://doi.org/10.1155/2012/831524.